NANO LETTERS

Letter

pubs.acs.org/NanoLett

Single-Crystal Diamond Nanowire Tips for Ultrasensitive Force Microscopy

Y. Tao[†,‡] and C. L. Degen*[,†]

[†]Department of Physics, ETH Zurich, 8093 Zurich, Switzerland

[‡]Department of Chemistry, Massachusetts Institute of Technology, Cambridge, Massachusetts 02139, United States

Supporting Information

ABSTRACT: We report the fabrication, integration, and assessment of sharp diamond tips for ultrasensitive force microscopy experiments. Two types of tips, corresponding to the upper and lower halves of a diamond nanowire, were fabricated by top-down plasma etching from a single-crystalline substrate. The lower, surface-attached halves can be directly integrated into lithographically defined nanostructures, like cantilevers. The upper, detachable halves result in diamond nanowires with a tunable diameter (50−500 nm) and lengths of a few microns. Tip radii were around 10 nm and tip apex angles around 15°. We demonstrate the integration of diamond nanowires for use as scanning tips onto ultrasensitive pendulum-style silicon cantilevers. We find the noncontact friction and frequency jitter to be exceptionally low, with no degradation in the intrinsic mechanical quality factor ($Q \approx 130\,000$) down to tip-to-surface distances of about 10 nm. Our results are an encouraging step toward further improvement of the sensitivity and resolution of force-detected magnetic resonance imaging.

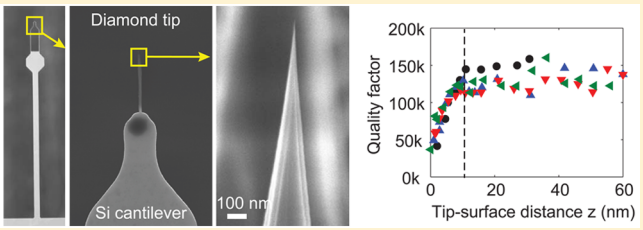

KEYWORDS: *Single-crystal diamond, nanowire, nanofabrication, noncontact friction, ultrasensitive force microscopy, nanomechanics*

Nanomechanical detection of ultrasmall forces is of considerable importance for the nanosciences, with applications in magnetometry of magnetic nanoparticles,[1−3] measurements of persistent ring currents,[4,5] fundamental tests of physics,[6,7] and various modes of force microscopy.[8] In particular, the detection of nuclear magnetic resonance signals using magnetic resonance force microscopy (MRFM)[9,10] requires sensitivity to forces in the zeptonewton to attonewton range (10^{-21}−10^{-18} N). Attonewton force detection has been demonstrated with several types of mechanical sensors, including silicon[11] and diamond[12] cantilevers, silicon nitride beams and membranes,[13,14] and silicon nanowires.[15] Excellent force sensitivities, of order zeptonewtons, were recently reported for trapped ions[16] and suspended carbon nanotube resonators.[17] With the exception of ref 15, all of these force sensitivities were demonstrated for freely vibrating beams or particles that were far (≳100 nm) from a surface.

It is well-known in the field of scanning probe microscopy that force sensitivities deteriorate as a tip is approached closely to a surface.[18,19] This undesired noncontact friction effect is due to dissipative forces between the moving tip and the surface. Several mechanisms were shown to contribute, including dielectric fluctuations,[20] radiative heat transfer,[21] and the presence of static or fluctuating surface charge.[22,23] Similar effects have also been observed with surface-electrode ion traps that are extremely sensitive to electrical fluctuations.[16,24] Due to the large number of interplaying mechanisms, a generally applicable microscopic theory of noncontact friction is currently lacking, and attempts at reducing it have more or less depended on empirical efforts. These efforts suggest that thin metal layers are effective at screening trapped charges and that surfaces with low dielectric constants and low loss tangents show the lowest friction. Friction is also reduced by minimizing the tip−surface interaction area, that is, by using tips with a small radius of curvature.

In this Letter, we combine, within a single experiment, all of the above ingredients required to suppress noncontact friction effects. We demonstrate that ultrasharp diamond nanowires (DNWs) can achieve exceptionally low noncontact friction and frequency jitter, with no measurable degradation within 10 nm from a gold surface.

Diamond has a low dielectric constant ($\epsilon_r = 5.7$) and low loss tangent ($\tan\delta \sim 2 \times 10^{-3}$ at 5 kHz),[25] forms no defect-rich native oxide, and is therefore an ideal candidate for a low-friction tip material. Moreover, it is mechanically robust and wear-resistant, which are important practical considerations with force microscopy. We have fabricated DNWs using masked etching of single-crystal substrates by inductively coupled plasma (ICP) reactive ion etching.[26−28] The advantage of top-down etching as compared to bottom-up methods[29,30] is that high quality and commercially available starting material can be used.

Two different masking schemes were found to be effective. In a first approach, we exploited intrinsic micromasking by surface

Received: July 22, 2015
Revised: October 19, 2015
Published: October 30, 2015

DOI: 10.1021/acs.nanolett.5b02885
Nano Lett. 2015, 15, 7893−7897

defects.[27] No surface patterning was applied, and commercially available optical-grade diamond (100) single crystals (ElementSix Ltd.) were introduced as-received into an ICP etcher. Etching for 30 min in 10 mTorr O_2 (30 sccm) using 2100 W ICP and 100 W bias powers led to the formation of randomly distributed pillar structures (Figure 1A–C).[31] The micromasking is most likely due to the unintended presence of impurities on the starting diamond substrate.[27] Indeed, we found that the pillar density can be controllably increased by deliberately introducing additional masking impurities, for example, by placing a glass coverslip (SiO_2) close to the diamond sample during the etching.[31]

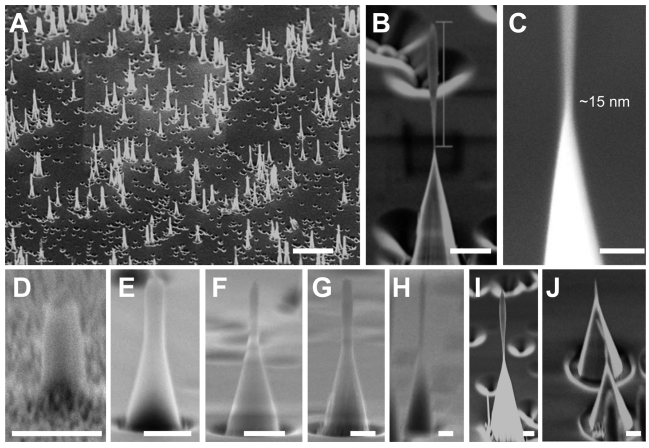

Figure 1. One-step fabrication of single-crystal diamond nanowires with ultrasharp tips. (A) Diamond nanowires formed on a (100) diamond substrate via ICP etching and intrinsic micromasking. Scale bar is 10 μm. (B,C) Zoom-in views of an individual nanowire and its ~15 nm thin waist region. Scale bar is 1 μm in C and 100 nm in D. (D–J) Time lapse of diamond nanowire growth after (D) 1 min, (E) 3 min, (F) 5 min, (G) 10 min, (H) 20 min, (I) 30 min, and (J) after cleavage of the top and bottom halves. Scale bars are 200 nm.

The pillars had two segments, with a pyramidal base connected to a nanowire-like tip via a thin waist (Figure 1(B)). Similar structures have been previously observed by Hausmann et al.[28] We believe that the bipartite shape of the pillars is controlled by a combination of chemical etching anisotropy, directional etching and electron shading effects. In some cases the lower pyramidal base distinctly showed what appeared to be crystallographic planes with a roughly 4-fold symmetry, suggesting the presence of chemical etching anisotropy. The upper nanowire-like segment, by contrast, was almost straight and thus formed by directional etching. Finally, waist formation can be explained by electron shading effects:[32] Bombardment by electrons and positive O_2^+ ions is expected to lead to negative charge build-up near the tip and positive charge build-up near the base,[31] which would bend the trajectories of the positive ions[33] and lead to the emergence of the waist. A time-lapse of the etching process (Figure 1D–I) shows that both the pyramidal base and nanowire tip grow at roughly the same rate.

The pillar structures were found to be stable when the waist diameter was above 10 nm. Additional ICP etching was used to completely erode the waist until the two segments separated (Figure 1J). Both segments—the substrate-bound pyramidal tip and the released nanowire—could then be considered for use in scanning probe applications.

We have also deterministically fabricated diamond nanowires starting from an electron-beam-defined alumina (Al_2O_3) etch mask.[28] Etching a patterned sample with 2500 W ICP and 40 W bias powers for 30 min led to an array of structures very similar to pillars obtained previously by stochastic micromasking (Figure 2A). This demonstrates that DNWs can be controllably produced at predefined locations. A noticeable difference was the thickness of the upper segment (typically a few hundred nanometers), which was much larger for the lithographically defined pillars due to the much larger size of the etch mask as compared to micromasking impurities (Figure 2B). Again, additional etching was used to controllably pinch off the waist to yield arrays of sharp tips with radii $\lesssim$10 nm (Figure 2C). The ability to controllably produce diamond tips at predefined locations is an important advantage of lithographically patterned nanowires. For example, tips could be directly integrated onto cantilevers to make monolithic diamond AFM probes. Single-crystal diamond cantilevers have recently been shown to exhibit outstandingly low internal mechanical friction.[12,34]

In order to assess the potential of diamond tips for sensitive force microscopy, we have measured their noncontact friction over a gold surface. For this purpose, a few nanowires were manually integrated on the ends of ultrasensitive silicon cantilevers whose mechanical frequency and quality factor could be accurately monitored. We have only tested the upper (released) halves of nanowires; however, we do expect the bottom halves to show similar dissipation properties since they are made of the same material and have similar tip geometry. The silicon cantilevers were of the kind used in recent nanomagnetometry[1−5] and mechanical spin detection[35,36] experiments (see Figure 3A), with a 4 K sensitivity of a few

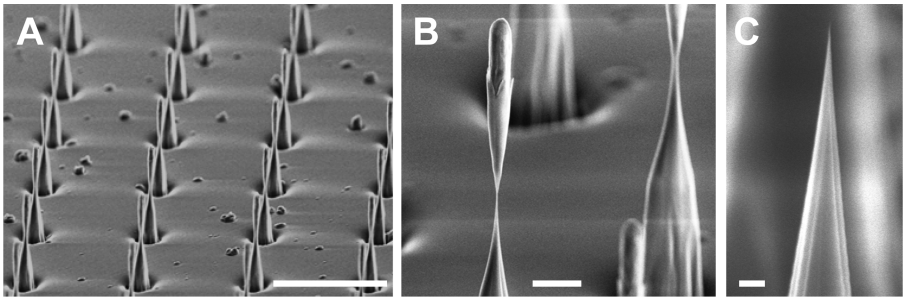

Figure 2. Lithographically defined single crystal diamond tips. (A) Regular array of tips formed after 30 min of ICP etching in an oxygen plasma. The scale bar is 10 μm. (B) Zoom-in view of a nanowire showing the thin waist before cleavage. The scale bar is 1 μm. (C) Cleavage results in sharp tips with radii of about 10 nm. The scale bar is 100 nm.

DOI: 10.1021/acs.nanolett.5b02885
Nano Lett. 2015, 15, 7893–7897

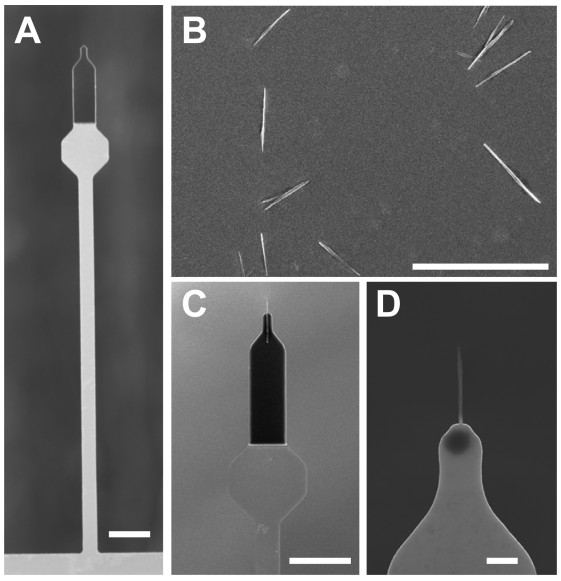

Figure 3. Integration of diamond nanowire tips on ultrasensitive silicon cantilevers. (A) Bare silicon cantilever with a nominal length of 90 μm, shaft width of 4 μm, and thickness of 135 nm. The scale bar is 10 μm. (B) Batch of DNWs transferred onto a Si substrate for manual pick-up. The scale bar is 10 μm. (C,D) Zoom-in onto the end region of two different cantilevers where DNW tips had been attached. Scale bars are 10 μm in C and 1 μm in D.

attonewtons per root Hz when far from a surface. The cantilevers were surface-passivated so as to increase the low-temperature quality factor from $Q \approx 50\,000$ to $Q \approx 130\,000$ (ref 37). DNWs were first transferred onto a piece of gel material (Gel-Pak-4) and then stamped onto a piece of silicon wafer (Figure 3B). Subsequently, individual nanowires could be picked up via van der Waals forces using a pulled glass tip and a micromanipulator. The nanowire was then deposited at the tip of the cantilever, where a dab of epoxy glue had been applied. Figure 3C–D shows examples of integrated DNW tips.

We have measured the noncontact friction of DNW tips using a pendulum configuration as illustrated in Figure 4A. Experiments were performed in a custom magnetic resonance force microscope[12] at a temperature of $T = 4$ K in a high vacuum environment. The tip was controllably approached to a gold surface via a piezo positioning system. The gold surface was produced epitaxially on c-cut single crystal sapphire following a procedure originally developed for the fabrication of single-crystal gold nanowires.[38] To determine the exact separation between the DNW tip and the surface, the cantilever was excited to a constant oscillation amplitude of about 5 nm-pk via feedback-controlled self-oscillation,[39] while the distance between the cantilever and the surface was slowly decreased. We defined the $z = 0$ point to be reached when the z-piezo extension caused the cantilever oscillation to stop due to the tip physically sticking to the surface. Repeated approach over the

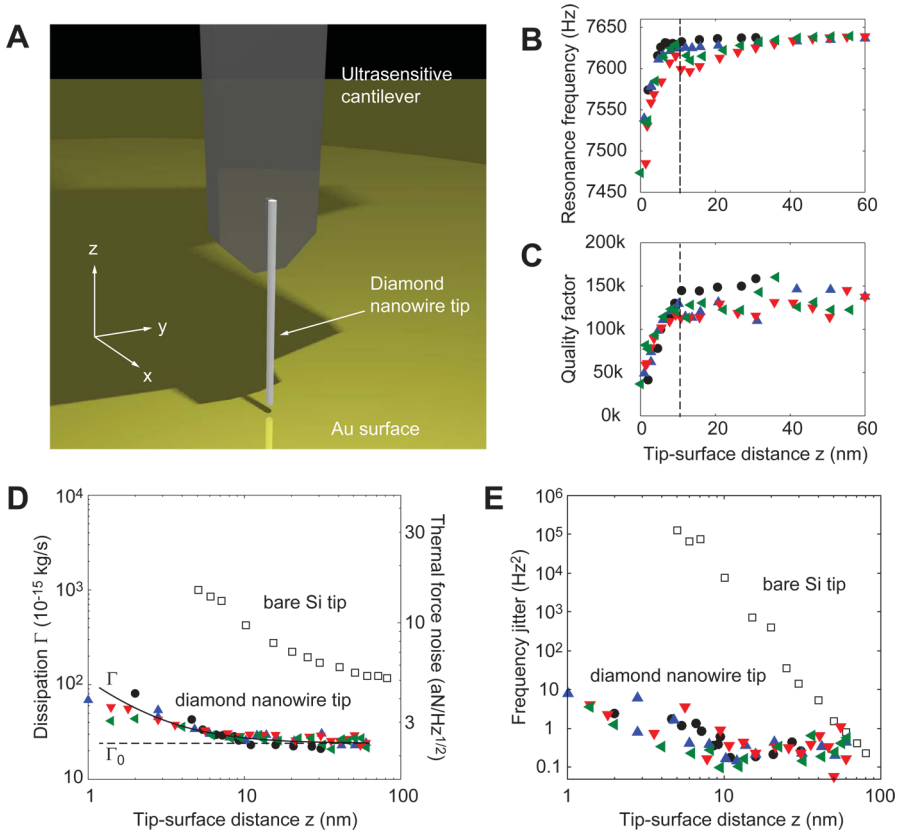

Figure 4. DNW tips experience very little noncontact friction. (A) Schematic illustration of the experimental configuration. The diamond-tipped silicon cantilever oscillates along x over a gold surface in a pendulum geometry. (B) Cantilever resonance frequency f_c as a function of tip–surface spacing z. Different symbols and colors represent measurements over different (x,y) locations on the surface. Vertical dashed line indicates $z = 10$ nm. (C) Mechanical quality factor Q as a function of z. (D) Mechanical dissipation Γ and inferred thermal force noise spectral density $S_F^{1/2}$ as a function of z. The dashed line indicates the intrinsic dissipation of $\Gamma_0 = 24 \times 10^{-15}$ kg/s. Solid line is a guide to the eye. Values for an equivalent cantilever without DNW tip are given for comparison (open symbols). (E) Frequency jitter $\langle \delta f_c^2 \rangle$ as a function of z.

DOI: 10.1021/acs.nanolett.5b02885
Nano Lett. 2015, 15, 7893–7897

same (x, y) location showed that the zero point was reproducible with a standard deviation of less than 1 nm.[31]

Figure 4B,C plot the resonance frequency f_c and the mechanical quality factor Q as a function of tip-to-surface separation z. The Q values were measured using the ring-down method.[40] The Q factor is the key quantity that determines the total mechanical dissipation $\Gamma = k_c(2\pi f_c Q)^{-1}$, where k_c is the spring constant (here $k_c \sim 160\ \mu$N/m), and the force noise spectral density $S_F = 4k_B T\Gamma$ of a mechanical sensor. Figure 4C shows that negligible changes in Q are observed up until the tip−surface distance decreased to below 10 nm. Remarkably, even just before reaching contact with the surface ($z \approx 1$ nm) the Q factor remained above 40 000. If we subtract the intrinsic mechanical dissipation, given by the baseline value of Γ_0 at large tip-to-surface separation (dashed line in Figure 4D), we find very low values of noncontact friction, about 3×10^{-15} kg/s at z = 10 nm and 9×10^{-15} kg/s at z = 5 nm. Comparable values of noncontact friction have to our knowledge only been observed with silicon nanowire resonators operating at high frequencies (~1 MHz)[15] where dissipative fluctuations are typically much lower.[24,41]

In addition to low noncontact friction, the DNW tips also showed very little jitter in the mechanical resonance frequency. Frequency jitter is an issue for ultrasensitive force measurements, because signal pickup requires a stable reference frequency and phase.[36] Moreover, frequency noise can parametrically upconvert to force noise and directly compromise the force sensitivity.[42] We have determined the frequency jitter $\langle \delta f_c^2 \rangle$ by calculating the variance of a series of f_c measurements with an effective bandwidth of ~1 Hz. As is evident from Figure 4E, no additional frequency noise was seen down to a tip-to-surface separation of $z \approx 10$ nm, and the frequency noise stayed below 10 Hz^2 even at the closest separation. This is in stark contrast to an equivalent cantilever without DNW tip (same figure).

The low levels of noncontact friction and frequency jitter observed in this work are encouraging steps toward nanomechanical detection of nuclear magnetism.[9,10,43] Force detection has played an important role in extending nuclear magnetic resonance to the nanometer scale[10] and has, for example, enabled the three-dimensional magnetic resonance imaging (MRI) of single virus particles with about 5 nm spatial resolution and a sensitivity of ~100 proton spins.[44] A key requirement for force-detected magnetic resonance is that the sample of interest can be approached as closely as possible to a magnetic gradient source, like a nanoscale ferromagnetic tip[45,46] or electromagnet.[15] The large magnetic gradient serves to generate a strong magnetic force on a spin, and it determines the achievable spatial imaging resolution. Gradients of up to G = 60 G/nm have recently been demonstrated at a tip-to-surface separation of $z \sim 25$ nm. Even higher gradients could be expected if the tip-to-surface spacing could be further reduced. Noncontact friction, however, impedes a reduction of z.

Our experiments suggest that $z \lesssim 10$ nm are possible with DNW tips at no cost in force sensitivity. Assuming that the gradient scales as $G \propto z^{-1}$ with distance z,[46,47] a gradient of order G = 150 G/nm can be expected at z = 10 nm with a tip similar to those in ref 46. Such high gradients have, in fact, been demonstrated for magnetic recording heads.[48,49] The force on a single proton spin in this gradient is about $F_{spin} \approx 0.21$ aN. This force can be compared with the minimum detectable force for the DNW-tipped cantilever of Figure 4 at z = 10 nm, which is about $S_F^{1/2} \approx 2.4$ aN/Hz$^{1/2}$ for T = 4 K. If we would allow the measurement to be carried out at T = 300 mK (ref 35), the minimum detectable force would improve to $S_F^{1/2} \approx 0.65$ aN/Hz$^{1/2}$. Such a sensitivity would bring single nuclear spin detection within the reach of acceptable measurement averaging times.[35]

Finally, DNW-tipped cantilevers could present a useful platform for measuring friction of single nanoobjects, like large biomolecules or quantum dots. Diamond surfaces are easily functionalized, and numerous methods exist for covalently attaching suitable organic linker molecules, such as streptavidin. Due to the sharp tip radii, it is conceivable to create tips with only a single molecule at the apex.[50] Such single molecule attachment would also be useful for mechanically detected MRI. Because the noncontact friction of organic materials is known to be small,[51] we do not expect attached single molecules to contribute significant friction with nuclear spin experiments where the standoff is of the order of a molecule's size.

In summary, we have presented a simple and effective method for the fabrication of single-crystal diamond nanowires (DNWs) with typical lengths of a few micrometers and diameters around 100 nm. Tip radii of the nanowires were of order 10 nm, making them suitable probes for scanning probe applications that require very sharp tips. We have assessed the noncontact friction and frequency jitter of DNW-equipped ultrasensitive silicon cantilevers, and find those to be exceptionally low, with no degradation down to tip-to-surface distances below 10 nm. Our results are an encouraging step toward further improvement of the sensitivity and resolution of force-detected magnetic resonance imaging.

■ ASSOCIATED CONTENT

Supporting Information

The Supporting Information is available free of charge on the ACS Publications website at DOI: 10.1021/acs.nanolett.5b02885.

Description of the diamond handling and etching process, transfer of diamond nanowires to cantilevers, and a description of the experimental apparatus for noncontact friction measurements (PDF)

■ AUTHOR INFORMATION

Corresponding Author

*E-mail: degenc@ethz.ch.

Notes

The authors declare no competing financial interest.

■ ACKNOWLEDGMENTS

The authors thank Urs Grob for the fabrication of ultrasensitive silicon cantilevers, and Christoph Keck, Alex Eichler, Brad Moores, Hiroki Takahashi, and Chih-Hsun Hsu for technical assistance and helpful discussions. This work has been supported by the ERC through Starting Grant 309301 and by the European Commission through the FP7-611143 DIADEMS programme.

■ REFERENCES

(1) Stipe, B. C.; Mamin, H. J.; Stowe, T. D.; Kenny, T. W.; Rugar, D. *Phys. Rev. Lett.* **2001**, *86*, 2874.

(2) Weber, D. P.; Ruffer, D.; Buchter, A.; Xue, F.; Russo-Averchi, E.; Huber, R.; Berberich, P.; Arbiol, J.; Morral, A. F. I.; Grundler, D.; Poggio, M. *Nano Lett.* **2012**, *12*, 6139−6144.

DOI: 10.1021/acs.nanolett.5b02885
Nano Lett. 2015, 15, 7893−7897

(3) Mehlin, A.; Xue, F.; Liang, D.; Du, H. F.; Stolt, M. J.; Jin, S.; Tian, M. L.; Poggio, M. *Nano Lett.* **2015**, *15*, 4839.
(4) Bleszynski-Jayich, A. C.; Shanks, W. E.; Peaudecerf, B.; Ginossar, E.; von Oppen, F.; Glazman, L.; Harris, J. G. E. *Science* **2009**, *326*, 272−275.
(5) Jang, J.; Ferguson, D. G.; Vakaryuk, V.; Budakian, R.; Chung, S. B.; Goldbart, P. M.; Maeno, Y. *Science* **2011**, *331*, 186−188.
(6) Lamoreaux, S. K. *Phys. Rev. Lett.* **1997**, *78*, 5−8.
(7) Chan, H. B.; Aksyuk, V. A.; Kleiman, R. N.; Bishop, D. J.; Capasso, F. *Science* **2001**, *291*, 1941−1944.
(8) Giessibl, F. *Rev. Mod. Phys.* **2003**, *75*, 949−983.
(9) Sidles, J. A.; Garbini, J. L.; Bruland, K. J.; Rugar, D.; Züger, O.; Hoen, S.; Yannoni, C. S. *Rev. Mod. Phys.* **1995**, *67*, 249.
(10) Poggio, M.; Degen, C. L. *Nanotechnology* **2010**, *21*, 342001.
(11) Stowe, T. D.; Yasumura, K.; Kenny, T. W.; Botkin, D.; Wago, K.; Rugar, D. *Appl. Phys. Lett.* **1997**, *71*, 288−290.
(12) Tao, Y.; Boss, J. M.; Moores, B. A.; Degen, C. L. *Nat. Commun.* **2014**, *5*, 3638.
(13) Teufel, J. D.; Donner, T.; Castellanos-Beltran, M. A.; Harlow, J. W.; Lehnert, K. W. *Nat. Nanotechnol.* **2009**, *4*, 820−823.
(14) Zwickl, B. M.; Shanks, W. E.; Jayich, A. M.; Yang, C.; Jayich, A. C. B.; Thompson, J. D.; Harris, J. G. E. *Appl. Phys. Lett.* **2008**, *92*, 103125.
(15) Nichol, J. M.; Hemesath, E. R.; Lauhon, L. J.; Budakian, R. *Phys. Rev. B: Condens. Matter Mater. Phys.* **2012**, *85*, 054414.
(16) Biercuk, M. J.; Uys, H.; Britton, J. W.; VanDevender, A. P.; Bollinger, J. J. *Nat. Nanotechnol.* **2010**, *5*, 646−650.
(17) Moser, J.; Guttinger, J.; Eichler, A.; Esplandiu, M. J.; Liu, D. E.; Dykman, M. I.; Bachtold, A. *Nat. Nanotechnol.* **2013**, *8*, 493−496.
(18) Denk, W.; Pohl, D. W. *Appl. Phys. Lett.* **1991**, *59*, 2171−2173.
(19) Grütter, P.; Liu, Y.; LeBlanc, P.; Dürig, U. *Appl. Phys. Lett.* **1997**, *71*, 279−281.
(20) Kuehn, S.; Loring, R. F.; Marohn, J. A. *Phys. Rev. Lett.* **2006**, *96*, 156103.
(21) Volokitin, A. I.; Persson, B. N. J. *Rev. Mod. Phys.* **2007**, *79*, 1291−1329.
(22) Stipe, B. C.; Mamin, H. J.; Stowe, T. D.; Kenny, T. W.; Rugar, D. *Phys. Rev. Lett.* **2001**, *87*, 096801.
(23) Siria, A.; Barois, T.; Vilella, K.; Perisanu, S.; Ayari, A.; Guillot, D.; Purcell, S.; Poncharal, P. *Nano Lett.* **2012**, *12*, 3551−3556.
(24) Labaziewicz, J.; Ge, Y.; Leibrandt, D. R.; Wang, S. X.; Shewmon, R.; Chuang, I. L. *Phys. Rev. Lett.* **2008**, *101*, 180602.
(25) Ibarra, A.; Gonzalez, M.; Vila, R.; Molla, J. *Diamond Relat. Mater.* **1997**, *6*, 856−859.
(26) Okuyama, S.; Matsushita, S. I.; Fujishima, A. *Langmuir* **2002**, *18*, 8282−8287.
(27) Ando, Y.; Nishibayashi, Y.; Kobashi, K.; Hirao, T.; Oura, K. *Diamond Relat. Mater.* **2002**, *11*, 824−827.
(28) Hausmann, B. J.; Khan, M.; Zhang, Y.; Babinec, T. M.; Martinick, K.; McCutcheon, M.; Hemmer, P. R.; Loncar, M. *Diamond Relat. Mater.* **2010**, *19*, 621−629.
(29) Sun, L.; Gong, J.; Zhu, D.; Zhu, Z.; He, S. *Adv. Mater.* **2004**, *16*, 1849−1853.
(30) Hsu, C.-H.; Cloutier, S. G.; Palefsky, S.; Xu, J. *Nano Lett.* **2010**, *10*, 3272−3276.
(31) See Supporting Information accompanying this manuscript.
(32) Giapis, K. In *Handbook of Advanced Plasma Processing Techniques*; Shul, R., Pearton, S., Eds.; Springer: New York, 2000.
(33) Burek, M. J.; de Leon, N. P.; Shields, B. J.; Hausmann, B. J. M.; Chu, Y.; Quan, Q.; Zibrov, A. S.; Park, H.; Lukin, M. D.; Loncar, M. *Nano Lett.* **2012**, *12*, 6084.
(34) Ovartchaiyapong, P.; Pascal, L. M. A.; Myers, B. A.; Lauria, P.; Jayich, A. C. B. *Appl. Phys. Lett.* **2012**, *101*, 163505.
(35) Rugar, D.; Budakian, R.; Mamin, J. H.; Chui, B. W. *Nature* **2004**, *430*, 329.
(36) Moores, B. A.; Eichler, A.; Tao, Y.; Takahashi, H.; Navaretti, P.; Degen, C. L. *Appl. Phys. Lett.* **2015**, *106*, 213101.
(37) Tao, Y.; Navaretti, P.; Hauert, R.; Grob, U.; Poggio, M.; Degen, C. L. *Nanotechnology* **2015**, *26*, 465501.
(38) Yoo, Y.; Seo, K.; Han, S.; Varadwaj, K. S. K.; Kim, H. Y.; Ryu, J. H.; Lee, H. M.; Ahn, J. P.; Ihee, H.; Kim, B. *Nano Lett.* **2010**, *10*, 432−438.
(39) Albrecht, T. R.; Grutter, P.; Horne, D.; Rugar, D. *J. Appl. Phys.* **1991**, *69*, 668.
(40) Mamin, H. J.; Rugar, D. *Appl. Phys. Lett.* **2001**, *79*, 3358.
(41) Yazdanian, S. M.; Hoepker, N.; Kuehn, S.; Loring, R. F.; Marohn, J. A. *Nano Lett.* **2009**, *9*, 2273−2279.
(42) Zhang, Y.; Moser, J.; Guttinger, J.; Bachtold, A.; Dykman, M. *Phys. Rev. Lett.* **2014**, *113*, 255502.
(43) Sidles, J. A. *Appl. Phys. Lett.* **1991**, *58*, 2854.
(44) Degen, C. L.; Poggio, M.; Mamin, H. J.; Rettner, C. T.; Rugar, D. *Proc. Natl. Acad. Sci. U. S. A.* **2009**, *106*, 1313.
(45) Poggio, M.; Degen, C. L.; Rettner, C. T.; Mamin, H. J.; Rugar, D. *Appl. Phys. Lett.* **2007**, *90*, 263111.
(46) Mamin, H. J.; Rettner, C. T.; Sherwood, M. H.; Gao, L.; Rugar, D. *Appl. Phys. Lett.* **2012**, *100*, 013102.
(47) Longenecker, J. G.; Mamin, H. J.; Senko, A. W.; Chen, L.; Rettner, C. T.; Rugar, D.; Marohn, J. A. *ACS Nano* **2012**, *6*, 9637−9645.
(48) Tsang, C.; et al. *IEEE Trans. Magn.* **2006**, *42*, 145.
(49) Tao, Y. *unpublished* 2015.
(50) Wilson, N. R.; Macpherson, J. V. *Nat. Nanotechnol.* **2009**, *4*, 483−491.
(51) Rugar, D.; Mamin, H. J. *Private communication*.

DOI: 10.1021/acs.nanolett.5b02885
Nano Lett. 2015, 15, 7893−7897